Phosphorescent white organic light-emitting devices with color stability and low efficiency decay by using wide band-gap interlayer*

CHEN Min(陈珉), **YU Jun-sheng**(于军胜)** , **LIN Hui**(林慧), **LEI Xia**(雷霞), **and WEN Wen**(文雯)
State Key Laboratory of Electronic Thin Films and Integrated Devices, School of Optoelectronic Information, University of Electronic Science and Technology of China, Chengdu 610054, China

(Received 14 August 2012)

High-performance phosphorescent white organic light-emitting devices (PhWOLEDs) with color stability and low efficiency decay are demonstrated by inserting wide band-gap materials between emitting layers. The two devices with N,N'-dicarbazolyl-3,5-benzene (mCP) and p-bis(triphenylsilyl)benzene (UGH2) as the interlayer exhibit both slight Commission Internationale del'Eclairage (CIE) coordinates variations of (± 0.010, ± 0.005) and (± 0.013, ± 0.006) in a wide voltage range, and low decay in current efficiency which shifts from the peak value 35.4 cd • A^{-1} and 27.4 cd • A^{-1} to 28.8 cd • A^{-1} and 23.5 cd • A^{-1} at 40000 cd • m^{-2}, respectively. The improvements are attributed to the charge carriers balance and the elimination of energy transfer loss by confining the carrier accumulation at the exciton formation interface through the interlayer.

Document code: A **Article ID:** 1673-1905(2013)01-0025-5
DOI 10.1007/s11801-013-2329-7

The development of white organic light-emitting devices (WOLEDs) is of central importance in scientific and industrial area spanning from full-color flat panel display and solid-state lighting[1]. White light emission can be obtained from phosphorescent, fluorescent, or hybrid phosphorescent-fluorescent materials[2-4]. Phosphorescent WOLEDs (PhWOLEDs) stand out because their internal quantum efficiency (IQE) is possibile to achieve up to 100 %. However, the problems in this architecture remain, such as the undesired color-shift over the entire process associated with the short operational lifetime of blue phosphor and the significant efficiency decay at high brightness due to the strong triplet-triplet annihilation or triplet-charge annihilation[5-7]. Accordingly, a lot of endeavors have been made to solve these issues, such as designing an exciton-confining structure[8], broadening the exciton formation zone[9], pin junction[10] architectures and manipulating singlet and triplet excitons within bipolar host[11]. However, we note that these methods need some complicated fabrication processes, which limits their further practical applications. In general, highly efficient WOLEDs with high color stability and low efficiency decay based on a simpler structure seem to be more promising.

Herein, we demonstrate PhWOLEDs with color stability and low efficiency decay by simply inserting wide band-gap interlayer between the blue and yellow emitting layers. The interlayers are the nominal wide gap hole-transporting material of N,N'-dicarbazolyl-3,5-benzene (mCP) and electron-transporting material of p-bis(triphenylsilyl)benzene (UGH2). With the analysis of device characteristics, the influence of the interlayer on the dynamics of charge carriers and triplet excitons is investigated.

PhWOLEDs in this paper have the structure as shown in Fig.1, which is ITO (150 nm)/1,1-bis[(di-4-tolylamino)phenyl] cyclohexane (TAPC) (30 nm)/mCP: 8 % iridium (III) bis (4,6-(di-fluorophenyl)-pyridinato-N,C2') picolinate (Firpic) (20 nm)/interlayer (x nm)/4,7-diphenyl-1,10-phenanthroline (BPhen): 6 % [2-(4-tertbutylphenyl) benzothiazolato-N,C2'] iridium (acetylacetonate) [$(t\text{-bt})_2$Ir(acac)] (15 nm)/BPhen (40 nm)/Mg: Ag (10:1, 200 nm). The devices are marked by A (without interlayer), B (interlayer stands for mCP, x= 3 nm) and C

* This work has been supported by the National Natural Science Foundation of China (Nos.60736005 and 60425101-1), the Foundation for Innovation Groups of NSFC (No.61021061), the Fundamental Research Funds for the Central Universities (No.ZYGX2010Z004), the SRF for ROCS, SEM (No.GGRYJJ08-05), and the Doctoral Fund of Ministry of China (No.20090185110020).
** E-mail: jsyu@uestc.edu.cn

(interlayer stands for UGH2, x= 0.2 nm), respectively. The mCP host doped with 8 % Firpic and the BPhen host doped with 6 % $(t\text{-}bt)_2Ir(acac)$ are blue and yellow phosphorescent emitting layers (EMLs), respectively. TAPC and BPhen were used as hole transporting layer (HTL) and electron transporting layer (ETL), respectively. The novel phosphorescent material $(t\text{-}bt)_2Ir(acac)$ was synthesized by our laboratory[12]. The characteristics of current-voltage-luminance (*J-V-L*) and electro-luminance (EL) spectra were measured with KEITHLEY-4200 semiconductor characterization system and an OPT-2000 spectrophotometer. All the measurements were performed at room temperature in ambient circumstances.

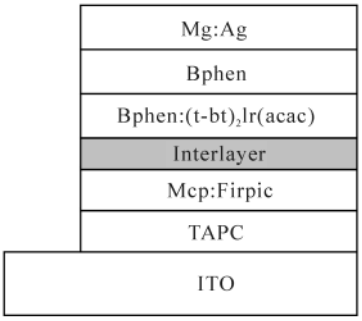

Fig.1 Structure of the prepared PhWOLEDs

Fig.2 summarizes the comparison of EL spectra among the PhWOLEDs. We can see that a major peak located at 470 nm and a shoulder peak at 494 nm are ascribed to Firpic emission, and a major peak located at 560 nm and a shoulder peak at 596 nm come from $(t\text{-}bt)_2Ir(acac)$. Generally, for the devices with two or more emitters, sequential energy transfer from the dopant with short wavelength to the dopant with long wavelength always dominates the emission mechanism, which exhibits weaker EL intensity in the short wavelength emission[13]. It is interesting to reveal the color shift of device A (without interlayer), which shows an obvious decrease in the yellow emission compared with the strong blue emission when the voltage is increased. Stable white emission is obtained in both device B (with 3 nm mCP interlayer) and device C (with 0.2 nm UGH2 interlayer). When the voltage is increased from 5 V to 13 V, the Commission Internationale del'Eclairage (CIE) coordinates shift from (0.373, 0.416) to (0.363, 0.411) with variations of (± 0.01, ± 0.005) for device B, and from (0.357, 0.410) to (0.344, 0.417) with variations of (± 0.013, ± 0.006) for device C, which are comparable to or even smaller than those of the high-performance single-EML or multi-EML WOLEDs reported before[14,15].

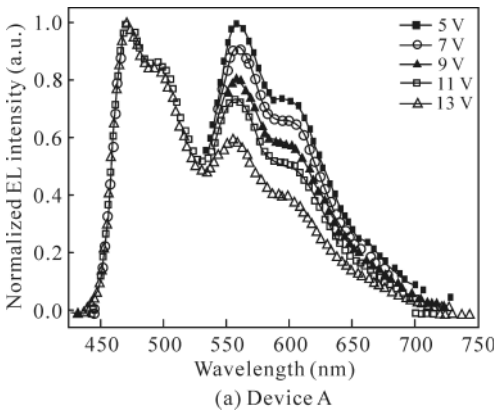

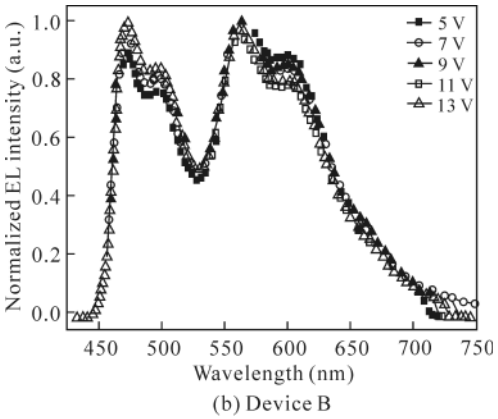

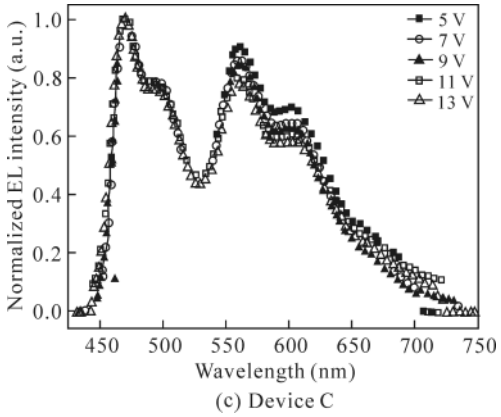

Fig.2 Normalized EL intensities of devices at the voltage varying from 5 V to 13 V

As shown in Fig.3, the current efficiency (CE) and power efficiency (PE) of device A are relatively high at low brightness, but they drop rapidly to the lowest values among the three devices at high brightness, which exhibits the highest efficiency decay. For example, the CE of device A drops sharply from the maximum of 31.7 cd • A^{-1} to 14.2 cd • A^{-1} at 40000 cd • m^{-2}, exhibiting decay in CE of 55% (calculated from the maximum to the value at 40000 cd • m^{-2}). The peak CE values of device B and device C are 35.4 cd • A^{-1} and 27.4 cd • A^{-1}, which slightly shift to 28.8 cd • A^{-1} and 23.5 cd • A^{-1} at 40000 cd • m^{-2}, with the decays of only 18 % and 14 %. These results demonstrate that the introduction of interlayer definitely improves device performance, which will be discussed as follows.

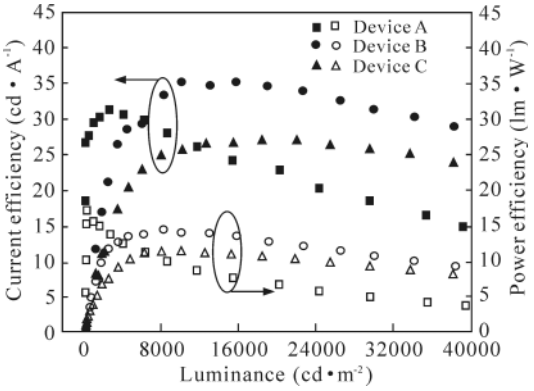

Fig.3 Current and power efficiencies of the PhWOLEDs

Fig.4 shows the external quantum efficiency (EQE) of the three devices and a blue (mCP: 8 % Firpic) OLED. Inset is the energy level diagram which is extracted from Refs.[12-16]. According to the energy level diagram, when there is no interlayer between the emitting layers, as the lowest unoccupied molecular orbital (LUMO) level difference between Bphen and Firpic (0 eV) is lower than that between Bphen and mCP (0.6 eV), most of the electrons can be resonantly transferred from Bphen to Firpic[16]. It has been demonstrated that the primary emission mechanism of mCP: Firpic host-guest system is energy transfer process[17], which indicates that energy-transfer process combining with direct exciton formation contributes to Firpic emission in our configuration. In addition, because of the dominant hole and electron transport characteristics of mCP[18] and Bphen[19], respectively, it can be assumed that the recombination zone is located in a narrow region near the blue emitting layer (B-EML)/yellow emitting layer (Y-EML) interface. Due to the hole blocking property of Bphen host and the higher-lying highest occupied molecular orbital (HOMO) (5.2 eV) of (t-bt)$_2$Ir(acac) compared with the HOMO (6.5 eV) of Bphen, deep hole trap can be formed on (t-bt)$_2$Ir(acac) dopant. Thus, the trapped holes combined with the scattered electrons on (t-bt)$_2$Ir(acac)

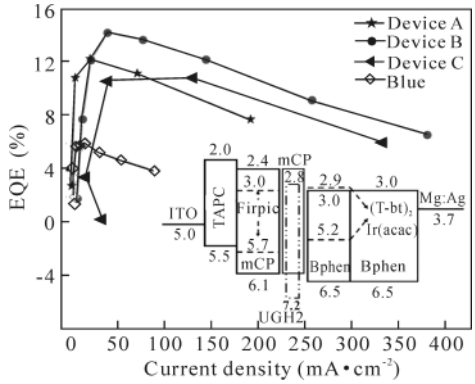

Fig.4 EQE values of the PhWOLEDs and blue (mCP: 8 % Firpic) OLED

result in the formation of exciton and the emission from (t-bt)$_2$Ir(acac). Combining all the reasons, we conclude that the main exciton formation zone of device A is located close to the B-EML/Y-EML interface. It is rather possible that the large number of excitons and polarons accumulated at this interface can result in strong triplet-triplet annihilation (TTA) and triplet-polaron annihilation (TPA)[20], leading to high efficiency decay of device A.

Given the distinct emission nature of each dopant in the devices, the EQE (ς_{ext}) of the PhWOLEDs can be simply described by the following equation[15]

$$\eta_{ext} = \eta_B(1-\chi_{trap}) + \eta_Y , \quad (1)$$

where ς_B is the EQE of Firpic-doped device, ς_Y is the quantum efficiency originated from yellow emission, and $\div_{trap}$ is the fraction of all electrically excited excitons which are formed directly on the (t-bt)$_2$Ir(acac) sites. By fitting the spectra of devices A−C to the EL spectra of the two individual dopants, we give the ratio of yellow and blue photon numbers ($R(P)_{yellow/blue}$) of our PhWOLEDs at various voltages, as shown in the inset of Fig.5. Combining the performance characteristics (ς_B) (Fig.4) of Firpic-doped blue device and $R(P)_{yellow/blue}$, we calculate a series of $\div_{trap}$ of our PhWOLEDs with the voltage from the first term in Eq.(1). Fig.5 shows $\div_{trap}$ plotted versus voltage.

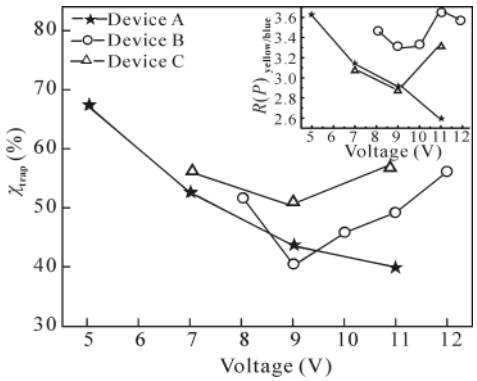

Fig.5 Fraction of trapped holes (χ_{trap}) as a function of applied voltage

According to the emission mechanism of our deivces, it can be seen that the change of spectra in emissive intensity of (t-bt)$_2$Ir(acac) with bias voltage should be related to how many hole carriers are directly trapped by (t-bt)$_2$Ir(acac) molecules at different electric fields. Obviously, $\div_{trap}$ of device A becomes smaller with increasing applied voltage, for example, from 67 % at 5 V to 39 % at 11 V, which leads to the unbalanced hole-electron on (t-bt)$_2$Ir(acac) and the less yellow emission compared with blue emission, consistent with the experimental results shown in Fig.2(a). It indicates that a lower

electric field is more favorable for the hole-trapping effect on $(t\text{-}bt)_2Ir(acac)$. The decrease of $\div_{trap}$ on $(t\text{-}bt)_2Ir(acac)$ can be explained by the enhanced electron mobility with increasing applied voltages. As Firpic is a well-known electron-transport triplet emitter[21], which means that more electrons could arrive at the B-EML through the BPhen channel to combine with the free holes, the amount of holes reaching the $(t\text{-}bt)_2Ir(acac)$ dopant can be reduced. The overall result is the continuous shift of the recombination distribution away from the main exciton formation zone towards the TAPC/B-EML interface, which results in a decrease in yellow emission relative to the strong blue emission with increasing voltage.

Considering the emission changing trend and the energy level offset among different materials, we suppose that controlling the charge carrier transport and exciton distribution by modifying the energy level alignment between the B-EML and Y-EML is the most important point. Because mCP is a good hole transporting material, and the LUMO offset (0.6 eV) between the mCP and BPhen can efficiently hinder the electron transporting into the B-EML, we introduce a thin mCP layer as the interlayer.

Device B with mCP interlayer exhibits an increasing trend on $\div_{trap}$ under high electric field, and the variation of $\div_{trap}$ is much smaller than that of device A. It suggests that the carrier distribution in the EMLs is controlled, and balanced hole-electron is obtained through the interlayer. When the 3 nm mCP is employed between the emitting layers, the large LUMO level difference can effectively limit the electrons from traveling to the B-EML, and then more electrons can be confined on the Y-EML side to balance the hole-electron ratio and increase the formation of excitons on $(t\text{-}bt)_2Ir(acac)$. At last, the efficient exciton recombination results in a stabler and stronger yellow emission. The balanced and stable white emission obtained in device B suggests that the main exciton formation zone has been broadened at both the B-EML/mCP interface and mCP/Y-EML interface. The broadened exciton recombination zone plays a role of suppressing the TTA effect due to the reduced exciton accumulation, leading to reduction of efficiency decay. Another probable reason for the low efficiency decay is an effective suppression of TPA effect at the B-EML/mCP interface for the decreased amount of electron polarons at this exciton formation zone[22]. However, as there is no difference of HOMO offset between the B-EML and the mCP interlayer, and the triplet energy of Firpic is higher than that of BPhen[23], a large amount of excitons in B-EML can facilely penetrate through the interlayer into the Y-EML, which increases the chance of non-radiative recombination and energy transfer loss. To further suppress the non-radiative recombination, we use a wider band-gap UGH2 as the interlayer to control the exciton diffusion.

In device C, the thin UGH2 layer plays a role of blocking hole trapped directly on $(t\text{-}bt)_2Ir(acac)$, since the HOMO level of UGH2 is much higher (1.1 eV) than that of mCP. But there is no influence on electron transport for the small LUMO level offset introduced by UGH2. Arguably, the higher injection barrier introduced by UGH2 can account for the difference in device performance. Given the large hole injection barrier, we introduce a much thinner UGH2 interlayer compared with mCP interlayer to guarantee hole carriers to arrive at the Y-EML. The EL spectra and the calculated $\div_{trap}$ of device C indicate that efficient excitons are formed on $(t\text{-}bt)_2Ir(acac)$. The hole injection barrier introduced by UGH2 can decrease the hole accumulation on $(t\text{-}bt)_2Ir(acac)$ which can help to balance electron-hole ratio and reduce the accumulation of hole polaron in the Y-EML at low voltage. Consequently, exciton quenching by hole polaron is suppressed, and the decrease of the yellow emission is prevented, which leads to stable white emission. On the other hand, electrons reaching the B-EML can be increased with increasing voltage. It is an effective way to increase the exciton formation and reduce the accumulation of polarons at the B-YEL/UGH2 interface by smartly increasing the amount of holes at this interface. Thus, the suppressed TPA effect is responsible for the reduced efficiency decay of device C. In addition, due to the large energy barrier (1.1 eV) between the B-EML and the much higher triplet energy level of UGH2 (3.5 eV), the exciton diffusion is well limited, and energy transfer loss is prevented, which results in a lower efficiency decay (around 14 %) compared with that of device B (around 18 %).

In summary, we fabricate two color-stable and low efficiency decay PhWOLEDs with mCP and UGH2 as the interlayer between the emitting layers, respectively. They exhibit stable white emission with slight CIE coordinates variations of ($\pm$ 0.01, $\pm$ 0.005) and ($\pm$ 0.013, $\pm$ 0.006) in a wide voltage range, respectively. The peak CE values of the two devices are 35.4 cd • A^{-1} and 27.4 cd • A^{-1}, which are slowly decreased to 28.8 cd • A^{-1} and 23.5 cd • A^{-1} at 40000 cd • m^{-2}. The work promotes a simple device configuration and an ingenious way to realize high-performance and color-stable WOLEDs.

References

[1] Qing-jin Qi, Xiao-ming Wu, Yu-lin Hua, Mu-sen Dong and Shou-gen Yin, Optoelectronics Letters **6**, 245 (2010).

[2] JIAO Zhi-qiang, WU Xiao-ming, HUA Yu-lin, BI Wen-tao, MU Xue, BAI Juan-juan and YIN Shou-gen, Journal of Optoelectronics • Laser **23**, 1252 (2012). (in Chinese)

[3] ZHAO Juan, YU Jun-sheng, LI Lu and JIANG Ya-dong, Journal of Optoelectronics • Laser **22**, 170 (2011). (in Chinese)

[4] QU Jian-jun, JIANG Quan, TAO Si-lu and GAN Yuan-yuan, Journal of Optoelectronics • Laser **22**, 56 (2011). (in Chinese)

[5] Juan Zhao, Junsheng Yu, Lei Zhang and Jun Wang, Physica B-Condensed Matter **407**, 2753 (2012).

[6] Fangchao Zhao, Zhiqiang Zhang, Yipeng Liu, Yanfeng Dai, Jiangshan Chen and Dongge Ma, Organic Electronics **13**, 1049 (2012).

[7] Baohua Zhang, Guiping Tan, Ching-Shan Lam, Bing Yao, Cheuk-Lam Ho, Lihui Liu, Zhiyuan Xie, Wai-Yeung Wong, Junqiao Ding and Lixiang Wang, Advanced Materials **24**, 1873 (2012).

[8] Shi-Jian Su, Eisuke Gonmori, Hisahiro Sasabe and Junji Kido, Advanced Materials **20**, 4189 (2008).

[9] Chih-Hung Hsiao, Yi-Hsin Lan, Pei-Yu Lee, Tien-Lung Chiu and Jiun-Haw Lee, Organic Electronics **12**, 547 (2011).

[10] Gregor Schwartz, Sebastian Reineke, Karsten Walzer and Karl Leo, Applied Physics Letters **92**, 53311 (2008).

[11] Xiao Yang, Hong Huang, Biao Pan, Matthew P. Aldred, Shaoqing Zhuang, Lei Wang, Jiangshan Chen and Dongge Ma, Journal of Physical Chemistry C **116**, 15041 (2012).

[12] J. Wang, Y. D. Jiang, J. S. Yu, S. L. Lou and H. Lin, Applied Physics Letters **91**, 1 (2007).

[13] Hsiao Chih-Hung and Lee Jiun-Haw, Journal of Applied Physics **106**, 024503 (2009).

[14] S. L. Lai, M. Y. Chan, M. K. Fung, C. S. Lee and S. T. Lee, Applied Physics Letters **90**, 203510 (2007).

[15] Qi Wang, Junqiao Ding, Dongge Ma, Yanxiang Cheng, Lixiang Wang and Fosong Wang, Advanced Materials **21**, 2397 (2009).

[16] Yang Jie and Shen Jun, Journal of Applied Physics **84**, 2105 (1998).

[17] R. J. Holmes, S. R. Forrest, Y. J. Tung, R. C. Kwong, J. J. Brown, S. Garon and M. E. Thompson, Applied Physics Letters **82**, 2422 (2003).

[18] Kim Sung Hyun, J. Jang and Lee Jun Yeob, Applied Physics Letters **90**, 223505 (2007).

[19] Lixin Xiao, Zhijian Chen, Bo Qu, Jiaxiu Luo, Sheng Kong, Qihuang Gong and Junji Kido, Advanced Materials **23**, 926 (2011).

[20] Sun Yiru and S. R. Forrest, Applied Physics Letters **91**, 263503 (2007).

[21] Wang Jun, Yu Junsheng, Li Lu, Wang Tao, Yuan Kai and Jiang Yadong, Applied Physics Letters **92**, 133308 (2008).

[22] N. Seidler, S. Reineke, K. Walzer, B. Lussem, A. Tomkeviciene, J. V. Grazulevicius and K. Leo, Applied Physics Letters **96**, 093304 (2010).

[23] Guohua Xie, Zhensong Zhang, Qin Xue, Shiming Zhang, Yang Luo, Li Zhao, Qingyang Wu, Ping Chen, Baofu Quan, Yi Zhao and Shiyong Liu, Journal of Physical Chemistry C **115**, 264 (2011).